

Department of Physics and Astronomy
University of Heidelberg

Bachelor Thesis in Physics
submitted by

Pascal Étienne Blessing

born in Stuttgart (Germany)

2016

Implementation of an Optical Dipole Trap for Lithium Atoms

This Bachelor Thesis has been carried out by Pascal Étienne Blessing at the
Max-Planck-Institute for Nuclear Physics in Heidelberg
under the supervision of

Priv.-Doz. Dr. Alexander Dorn

Second reviewer
Prof. Dr. Thomas Pfeifer

Abstract

Optical dipole traps are often used to provide an ultra-cold atom gas. Red detuned dipole traps are in principal rather easy to implement since they only consist of a focussed laser beam and without great complexity a potential minimum can be achieved. Bigger issues are the optimization of these traps as the intensity noise of the cw laser needs to be stabilized and thermal effects due to the high laser power traveling through the optical elements need to be minimized.

Zusammenfassung

Optische Dipolfallen werden häufig verwendet, um ein ultra-kaltes Atomgas bereitzustellen. Rot verschobene Dipolfallen sind prinzipiell eher einfach umzusetzen, da sie nur aus einem fokussierten Laserstrahl bestehen und ohne große Komplexität ein Potential-Minimum erzielt werden kann. Größere Probleme stellt die Optimierung dieser Fallen dar, da hierfür das optische Rauschen des CW-Lasers stabilisiert und thermische Effekte, die durch die hohe Laserleistung entstehen, die die optischen Elemente durchquert, minimiert werden muss.

Contents

1	Introduction	5
2	Theory of an Optical Dipole Trap	7
2.1	Dipole Potential	7
2.2	Loading the Dipole Trap from the MOT	8
2.3	Evaporative Cooling	9
2.4	Laser-noise-induced Heating	9
3	Theory of a PID controller	10
4	Intensity Stabilization	12
4.1	First Steps	12
4.2	ADwin-Pro II as PID-Controller	14
4.3	Red Pitaya as PID-Controller	16
4.4	Analog PID Controller	28
5	Possible Solutions	30
5.1	Thermal Lensing	30

Chapter 1

Introduction

In this experiment we need an initial momentum which is almost zero. Movement directly corresponds to temperature. The more the atoms move, the higher is the temperature of the gas.

Here we use a highly energetic pulsed laser, which sends out a light pulse of the length of a few femto seconds at a frequency of 1 Hz. An electron gets simply kicked out of the electron shell by an incoming photon and the atom is ionized. It is also possible that an electron of the inner shell gets kicked out and on its way out it simply hits another electron so the atom is double ionized. This laser sends out a lot of these highly energetic photons during one pulse, which means that many atoms are ionized at the same time. At this ultra low temperature the density is really high. These atoms are kept in a vacuum chamber in a Reaction Microscope. A Reaction Microscope consists of a magnetic field and two electrodes which force the ions to fly in one and the electrons to fly in the other direction. On each side there are detectors which can detect the position and the momentum of the particle. This information only is useful for fundamental physics, if the initial momentum of the atoms in the target is really small and therefore negligible.

A Magneto-Optical Trap (MOT) is used in order to get a really cold target in the first place. From there we transfer the atoms in an optical dipole trap. We use an Ytterbium Fiber Laser YLR-200-LP from IPG Photonics at a wavelength of $\lambda = 1070 \text{ nm}$, up to 200 W, linearly polarized [9]. For the intensity stabilization it would not be fast enough to modulate the laser current, so we use an Acousto-Optic Modulator (AOM), the MQ40-A3-L1064-W from AA Opto-Electronic [7], which is driven by an RF Driver, QMODP1-02, also from

AA Opto-Electronic [8]. An AOM consists of a piezo and a crystal. A piezo increases in size when voltage is applied to it. When this voltage oscillates at a high frequency, sound waves travel the crystal which means that there are density differences moving from one side to the other in the crystal. This affects the incoming laser beam so that on the other side of the crystal there will be a pattern with the 0. order at the frequency of the laser light $\omega = \omega_0$ and in the 1. order the frequency is $\omega = \omega_0 + \omega_{AOM}$ and in the n. order $\omega = \omega_0 + n \cdot \omega_{AOM}$ for $n = 0, \pm 1, \pm 2, \dots$. By varying the amplitude of the radio frequency on the piezo the intensity of the laser in the 1. order can be varied. This process is combined with a PID controller which gets a setpoint and then controls the amplitude just right so that the laser intensity stays stable. This stabilization is important because the atoms in the trap tend to heat up rather quick due to noise-induced heating (as will be discussed later) which would lead to a higher temperature and trap loss.

Chapter 2

Theory of an Optical Dipole Trap

2.1 Dipole Potential

The electric field \mathbf{E} of the laser light, in which an atom is placed, induces a dipole moment \mathbf{p} , oscillating at the driving frequency ω . The electric field is noted the following

$$\mathbf{E}(\mathbf{r}, t) = \hat{\mathbf{e}}E(\mathbf{r})\exp(-i\omega t) + c.c. \quad (2.1)$$

with the unit vector $\hat{\mathbf{e}}$ pointing in the direction of the polarization, while the induced atomic dipole moment then is

$$\mathbf{p}(\mathbf{r}, t) = \hat{\mathbf{e}}p(\mathbf{r})\exp(-i\omega t) + c.c. \quad (2.2)$$

where the amplitudes \tilde{E} and \tilde{p} are related by

$$\tilde{p} = \alpha\tilde{E} \quad (2.3)$$

Here α is the *complex polarizability*, which is dependent on the driving frequency ω . The resulting interaction potential of the induced dipole moment is

$$U_{dip} = -\frac{1}{2}\langle\mathbf{p}\mathbf{E}\rangle = -\frac{1}{2\epsilon_0 c}Re(\alpha)I \quad (2.4)$$

where $\langle\mathbf{p}\mathbf{E}\rangle$ denotes the time average over the two oscillating terms. The factor $\frac{1}{2}$ is there, because it is an induced potential and not a permanent one. The right hand side of the equation is simply derived from $I = 2\epsilon_0 c|\tilde{E}|^2$. The dipole

force therefore is

$$\mathbf{F}_{dip}(\mathbf{r}) = -\nabla U_{dip}(\mathbf{r}) = \frac{1}{2\epsilon_0 c} \text{Re}(\alpha) \nabla I(\mathbf{r}) \quad (2.5)$$

Therefore the resulting dipole force is a conservative force, proportional to the intensity gradient field.

The Lithium atoms are approximated as a two-level-atom with a ground state and an excited state. The polarizability α can be calculated by integration of the equation of motion $\ddot{x} + \Gamma_\omega \dot{x} + \omega_0^2 x = -eE(t)/m_e$ for the driven oscillation of the electron in the electron shell.

$$\alpha = \frac{e^2}{m_e} \frac{1}{\omega_0^2 - \omega^2 - i\omega\Gamma_\omega} \quad (2.6)$$

with the elementary charge e , the electron mass m_e and the scattering rate Γ . In 'Optical dipole traps for neutral atoms' from Grimm and Weidemüller [1] there are more detailed explanations and more calculations.

With more assumptions, some approximations and some transformations we get a dipole potential dependent on the detuning $\Delta = \omega - \omega_0$ of the dipole laser.

Dipole trapping in far detuned laser fields - also called far-off resonance traps (FORT) - can be understood on the basis of these two equations

$$U_{dip}(\mathbf{r}) = \frac{3\pi c^2}{2\omega_0^3} \frac{\Gamma}{\Delta} I(\mathbf{r}) \quad (2.7)$$

$$\Gamma_{sc}(\mathbf{r}) = \frac{3\pi c^2}{2\hbar\omega_0^3} \left(\frac{\Gamma}{\Delta}\right)^2 I(\mathbf{r}) \quad (2.8)$$

So if the detuning Δ is negative, $\omega < \omega_0$ as for red detuned laser light, we end up having a potential minimum in which the atoms will be trapped. The dipole potential therefore scales as I/Δ , whereas the scattering rate scales with I/Δ^2 . Far red detuned optical dipole traps have a high intensity and also a high (negative) detuning, so that the dipole potential is quite high, but the scattering rate Γ_{sc} is kept as low as possible. [1]

2.2 Loading the Dipole Trap from the MOT

The atoms are pre-cooled and trapped by a setup including a *Zeeman Slower* and a *Magneto-Optical Trap (MOT)*. The temperature is in a range of 100–1000 μK . Niels Kurz measured $(180 \pm 2) \mu K$ at a ballistic expansion measurement. First

of all the laser beams of the MOT and the Zeeman Slower are turned off and the *Ytterbium Fiber Laser* (which from now on will be referred to 'dipole laser' as it is usual in lab slang) is turned on to 200 W while the magnetic quadrupole field is still left on during the transition into the optical dipole trap. When the dipole laser is turned on, the magnetic field can be ramped down. Then the laser intensity is reduced to 30 W. These steps happen in the order of magnitude of 1-1000 μ s.

2.3 Evaporative Cooling

The laser intensity is ramped down to 30 W in order to perform forced evaporative cooling. This effect sounds fancy and happens all the time. The highly energetic atoms leave the trap as they have enough energy to overcome the potential barrier. When the trapping potential is reduced, the 'fast' atoms are even more likely to overcome the potential barrier, because it is lower now. After this procedure probably > 99.9 % of the atoms have left the trap and only the ultracold 'slow' atoms are left in the trap. Temperatures down to the nK-regime can be reached with this technique.

2.4 Laser-noise-induced Heating

Due to optical noise in the laser light the atoms in the trap can be heated. The time in seconds to increase the average energy by a factor e is called the energy e-folding time T_I . The fractional fluctuation in the laser intensity is given by

$$\epsilon(t) = \frac{I(t) - I_0}{I_0} \quad (2.9)$$

When the intensity noise would evenly be distributed over a 40-kHz bandwidth, the rms fractional intensity noise $\langle \epsilon(t) \rangle = \epsilon_0$ must be better than $\epsilon_0 = 6 \cdot 10^{-4}$ to reach an energy e-folding time of $T_I = 100$ s [14]. For shorter times T_I and smaller bandwidths it does not have to be that well smoothed.

The noise in the kHz regime still has to be suppressed in order to avoid rapid heating in our dipole trap.

Chapter 3

Theory of a PID controller

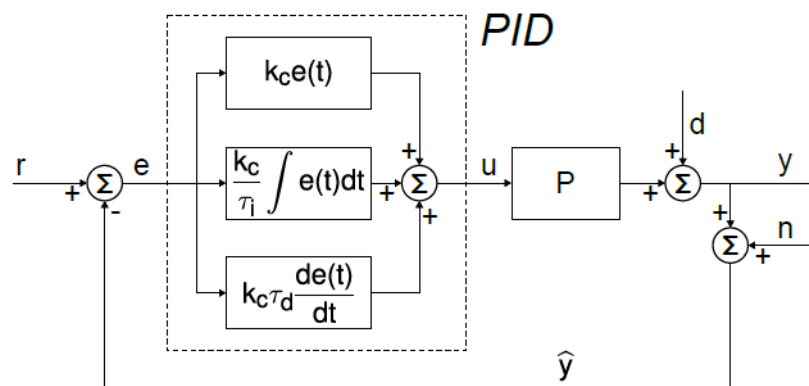


Fig. 00 Block diagram of a PID feedback loop. The user puts setpoint r . Output y of Process P is measured with a sensor adding noise n . The sum \hat{y} is then subtracted from r to get error e . This is fed to the PID controller. In response it takes control action u to obtain $y = r$ even if there is an unpredictable disturbance d in y .¹

There are three parameters of a PID controller: The proportional gain, the integral gain and the derivative gain. Let us begin straightforward: The controlled variable y can either be higher or lower than the setpoint r . Using only the proportional gain would make the output proportional to the input and match the setpoint exactly but stay at $y = e \cdot k_c = r \cdot \frac{k_c}{k_c - 1}$.

¹Seidler, F., (2015). Digital high bandwidth feedback controller. Master thesis. Fig. 2.1, page 3.

To counteract this limit we apply integral action. This part will keep rising, increasing y and decreasing e , until $e = 0$. The odd side is, that it has a time constant τ_i limiting the reaction time. Both of these parts put together form a PI controller, which is used in most application. The D-Part is used for rapid changes since its contribution will be largest for steep slopes. On the other hand it also creates an overshoot if the change is faster than the response time implied by the derivative time constant τ_d . In our case we probably won't need the D-Part since it would be easier to keep the control time as small as possible and then let the P- and I-Part do the rest. The control time needs to fit $1/f_{max}$ with f_{max} the maximum frequency of the noise we want to suppress. Then the deviation from the setpoint will be measured for this time interval and afterwards the signal u will be changed to the right value in order to counteract to the disturbance d . This is important because of the reaction time of the Process P . Rapid fluctuations, which are probably coming from the disturbance n (high frequency sensor noise).

Chapter 4

Intensity Stabilization

4.1 First Steps

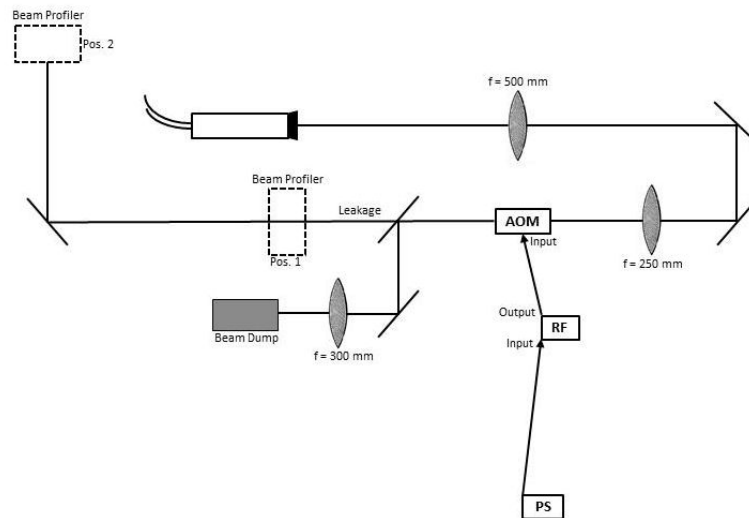


Fig. 01 Setup for the implementation of the AOM.

At first the beam diameter had to be decreased to fit the laser beam through the AOM. This was done by using two lenses in a distance of 750 mm as a telescope (see Fig. 01). About 2 meters behind the AOM we put a Beam Profiler in order to optimize the beam diameter ($1/e^2$). To the image of the beam a gaussian function has been fit. While watching the beam profile one was able to

adjust the two lenses in x- and y-direction while checking if the beam shape is round and also, the more important part, to adjust the latter lens in z-direction for the diameter needed. We then put the Beam Profiler directly (about 5 cm) behind the AOM. When there was a perfect gaussian beam with a beam diameter of 2.5 mm the lenses were in the right position. For implementing the AOM one had to perform a beamwalk to optimize the 1. order. We achieved to put 75 % in the 1. order which should be good enough since the data sheet refers to 80 % for the 1. order with a running AOM compared to the 0. order without the RF power on. It was not really a good idea to use the infrared-cards (which emit red light due to fluorescence effects) because they started to burn rather quickly due to the immense laser power of the dipole laser. After having adjusted that, the photodiode was put into operation and the following set-up was built.

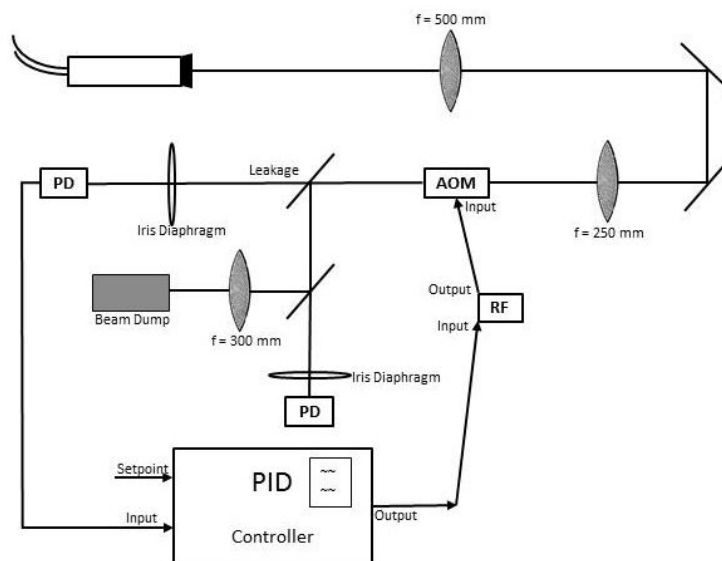


Fig. 02 PID control setup with iris diaphragms in front of the photodiode so that just the 1. order is detected on this photodiode. The second photodiode was used for out-of-loop monitoring purposes for the spectrum analyzer and the oscilloscope.

The responsivity of the photodiode had to be good at a wavelength of 1070 nm, because we can only use the leakage of the laser beam. The full power at which we stabilize the dipole laser is around 30 W and therefore the power of the

transmitted laser beam is at an order of magnitude of around 1 to 6 mW. There were two photodiodes in stock, which fulfilled these criteria. Both of them with a built-in amplifier - one of them with a fixed gain and the other one with 8 x 10 dB steps. Depending on the gain setting the bandwidth changes which is directly connected to the rise time via

$$t_r = \frac{0.35}{f_{BW}}$$

The following table contains values taken from the data sheet of the PDA10A (Thorlabs).

Setting [dB]	Rise Time	Bandwidth [Hz]
0	36 ns	$1.0 \cdot 10^7$
10	65 ns	$5.5 \cdot 10^6$
20	360 ns	$1.0 \cdot 10^6$
30	1.4 μs	$2.6 \cdot 10^5$
40	2.4 μs	$1.5 \cdot 10^5$
50	8 μs	$4.5 \cdot 10^4$
60	33 μs	$1.1 \cdot 10^4$
70	72 μs	$5.0 \cdot 10^3$

Tab. 01 Rise- and falltime of the photodiode PDA10A-EC

Now we know that the settings above 20 dB would slow our control circuit down too much. The photodiodes both give an output signal between 0-10 V.

The voltage range for the analog input of the RF Driver is 0-5 V. Via this signal the amplitude of the RF signal is modified as can be seen in Fig. 09. The intensity in the 1. order directly corresponds to the amplitude-modulated RF-signal on the piezo and to the sound wave in the crystal, respectively.

4.2 ADwin-Pro II as PID-Controller

We now are ready to integrate the PID controller in the set-up. At first we used the new ADwin-Pro II which came with a sample program, we had to modify a little bit. The voltage range for the analog inputs is -10 to 10 V, same for the outputs.

Unfortunately the working capacity of the ADwin reached 85% at the given cycle time. As can be seen in the following figures, the step size of the output was

quite big (0.3 V) and also the ADwin only changed the output voltage every 10 μ s.

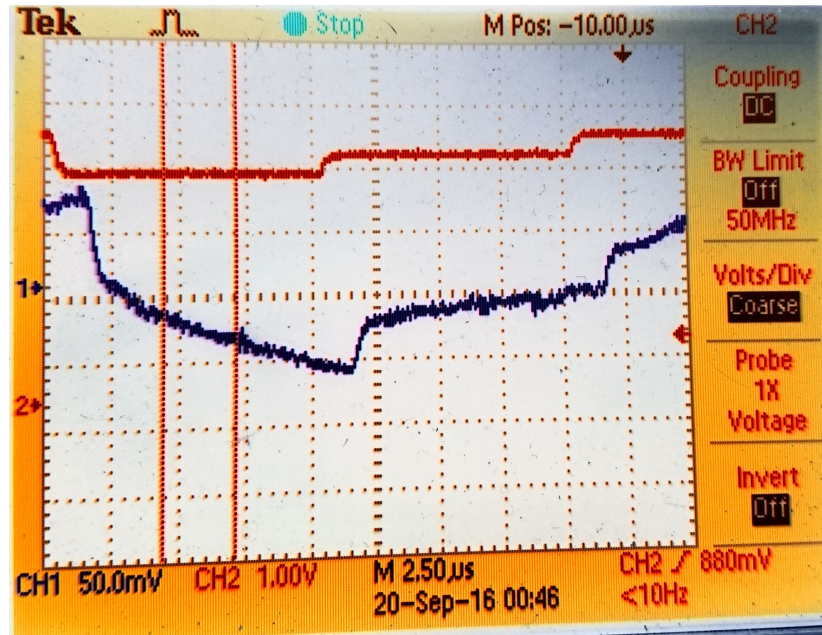


Fig. 03 The blue line (channel 1) shows the signal of the photodiode while the number 1 is set to the desired value of the control circuit. The red line (channel 2) shows the output signal of the ADwin.

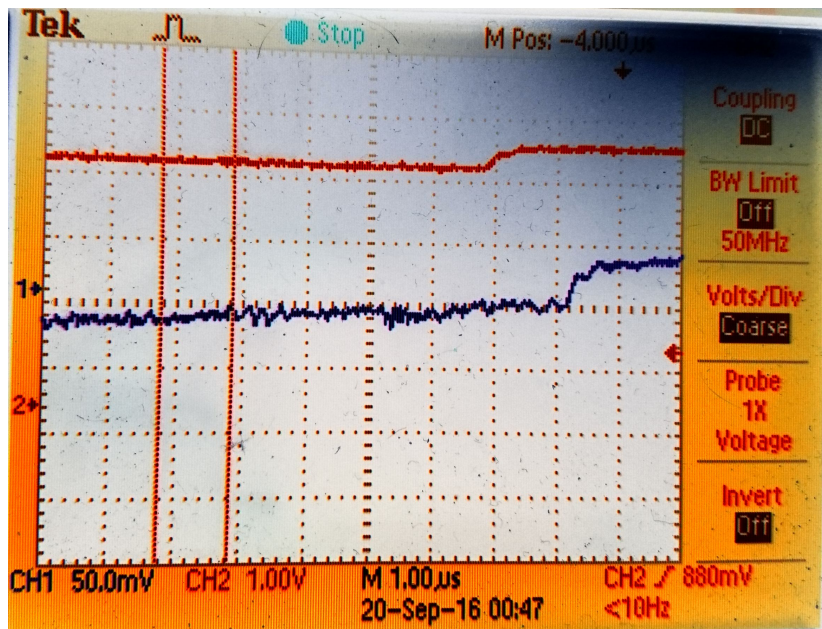


Fig. 04 Here we have the same setup as in Fig. 03, simply zoomed in that one can read out the reaction time of our set-up. The time between a change in the output signal of the ADwin and the responding change on the photodiode is a bit more than $1 \mu s$.

Since it should be possible to compensate optical noise in the order of magnitude of a few hundred kHz , this reaction time is good enough.

Nevertheless we could not use the ADwin for that purpose, because on the one hand the time to decide, whether the control signal should go up or down, was too long and on the other hand the initial main function of the ADwin is to control the whole experiment which might be difficult, when already 85% of the working capacity are needed for the intensity stabilization.

4.3 Red Pitaya as PID-Controller

The Red Pitaya board is well known for fast ADCs (analog to digital converters) and DACs. It has a sample rate of 125 Msps (Mega-samples per second). [13]

The output voltage range of the Red Pitaya is -1 to 1 V, while the input range can be set to either -1 to 1 V (jumper setting on Low) or to -20 to 20 V (jumper setting on High). The input range of the RF-Driver is 0-5V. So there

were two possibilities. Either using an amplifier at the RP output or adding a DC offset to the aforementioned output signal. An amplifier always has some kind of high-pass or low-pass filter. Also the noise at the RP output would be amplified. Florian Seidler of the University of Bonn measured the noise at the RP output with a spectrum analyzer (Fig. 05)

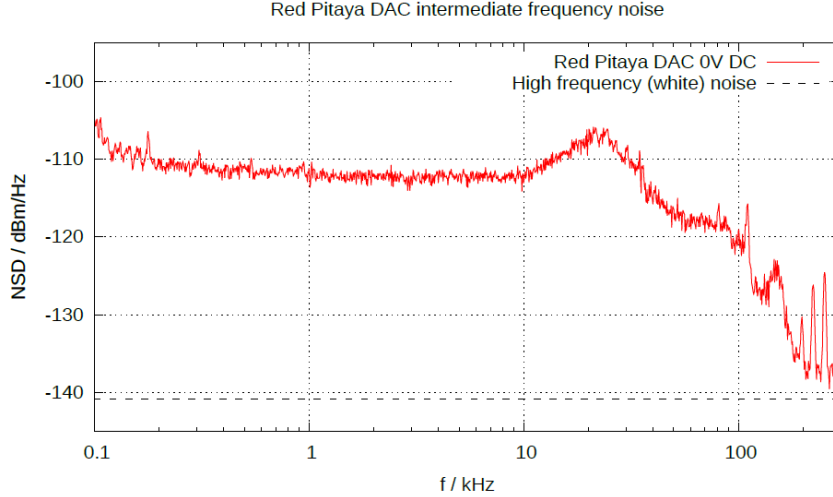


Fig. 05 Output noise produced by the DAC at frequencies between 100 Hz and 300 kHz. Note that this graph uses a logarithmic frequency scale. Above 300 kHz the amplifier used for this measurement distorts the results. Also note that this is not $1/f$ noise, which would resemble a linear function with a slope of 20 dB per decade.¹

An amplifier would also increase the step size (there are noticeable steps because it is a digital set-up) of the output signal. The main task of the Red Pitaya in this case is to compensate the optical noise of the dipole laser, so it would be the better idea to add a DC offset to the output offset so the RP just needs to modulate the signal around $0V \pm 20mV$. It would even be helpful to use an attenuator at the output to decrease the step size and to increase the operating range of the RP to $\pm 200mV$. On the contrary, the step size has not turned out to be a problem yet. In order to extend the output voltage of the RP to 3-5V we simply added 4V by connecting a power supply (4V) in series with the RP output, which gives us $U_{sum} = U_{RP} + U_{PS}$ after Kirchhoff's voltage law.

¹Seidler, F., (2015). Digital high bandwidth feedback controller, Master thesis. Fig. 4.4, page 30.

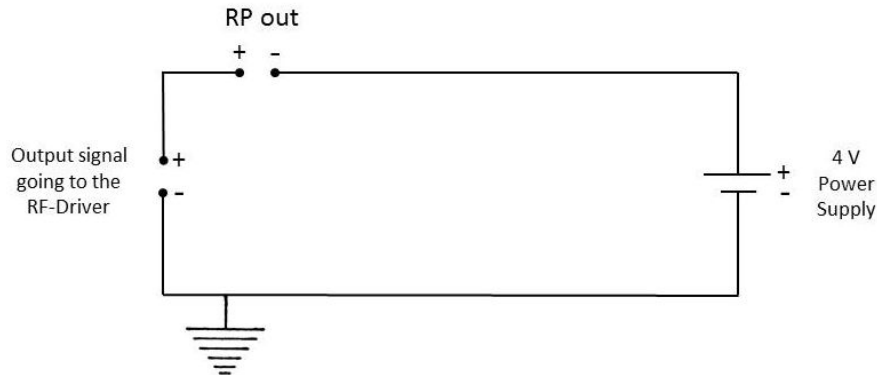


Fig. 06 The output signal gives us U_{sum} , when these two signals are added.

The ground of the Red Pitaya was grounded via the shielding of the ethernet cable so we disconnected it from the RP board. This did not affect the signals inside of the cable since they are sent as a potential difference between two pins and not between one pin and the ground (shielding of the cable) as it is done with BNC cables. After having fulfilled the hardware requirements, we started the software ('Oscilloscope & PID controller' to be found at the application market on bazaar.redpitaya.com). It was nearly impossible to find the right parameters by simply checking if the RMS error of the output signal at the photodiode was decreased. We needed an additional disturbance to check, whether the program is working in general and also to find the right parameters for K_P, K_I and K_D , while we set $K_D = 0$ for most of the time. At first the output of a signal generator has been added to the circuit like it is shown in Fig. 07.

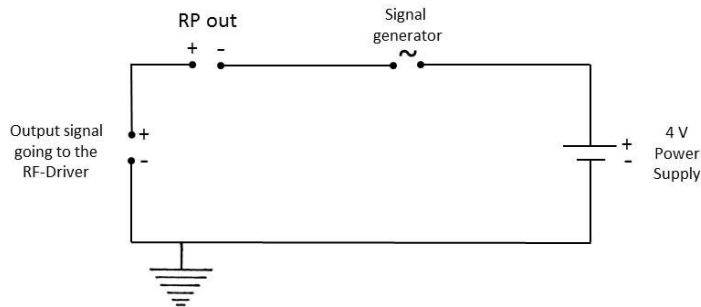


Fig. 07 An electrical disturbance signal is added to the Red Pitaya. This way, the board can directly try to compensate the oscillation from the signal generator. The input of the Red Pitaya is still the photodiode.

In this way the RP was able to compensate a sine signal of up to 4.0 kHz. This is definitely not fast enough. One problem was the rise time of the whole setup.

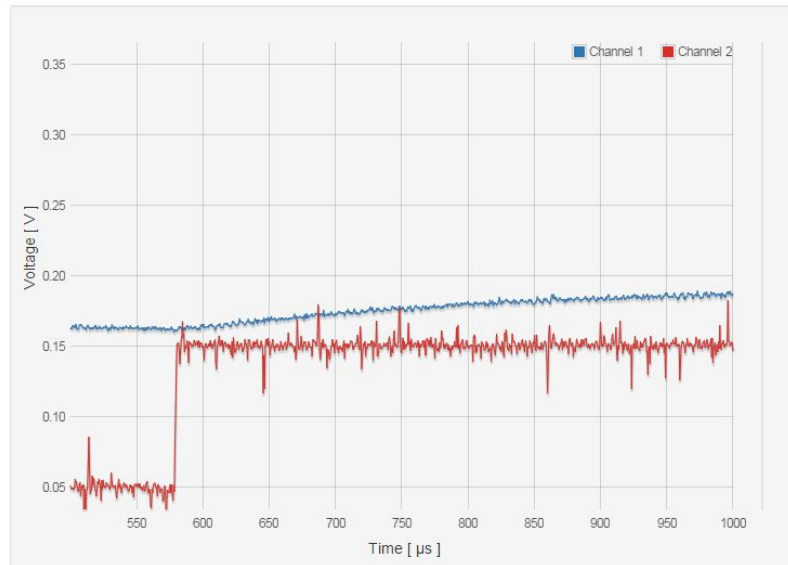


Fig. 08 The red line is the output signal of the RP and the blue one is the signal from the photodiode.

Afterwards a similar graph was taken at the RP Driver (CH1: signal of the RP, CH2: power monitoring output of the RF Driver). In the data sheet of the RF Driver the rise time is 34 ns. Another problem was that the signal from

the power supply contained a lot of high frequency noise (these huge 'spikes' in the red line). This noise came from the long banana cables which then were replaced by BNC cables with a grounded shielding. To be absolutely sure the RF Driver is not broken, we connected the output of the RF Driver over a Tee connector with both the oscilloscope ($1\text{ M}\Omega$ impedance) and the AOM ($50\ \Omega$ impedance) so that the main power (of the 30 W from the RF Driver) will be reflected to the AOM instead of going back to the RF Driver. It happened on Alexander's behalf and turned out to work perfectly and nothing was destroyed.

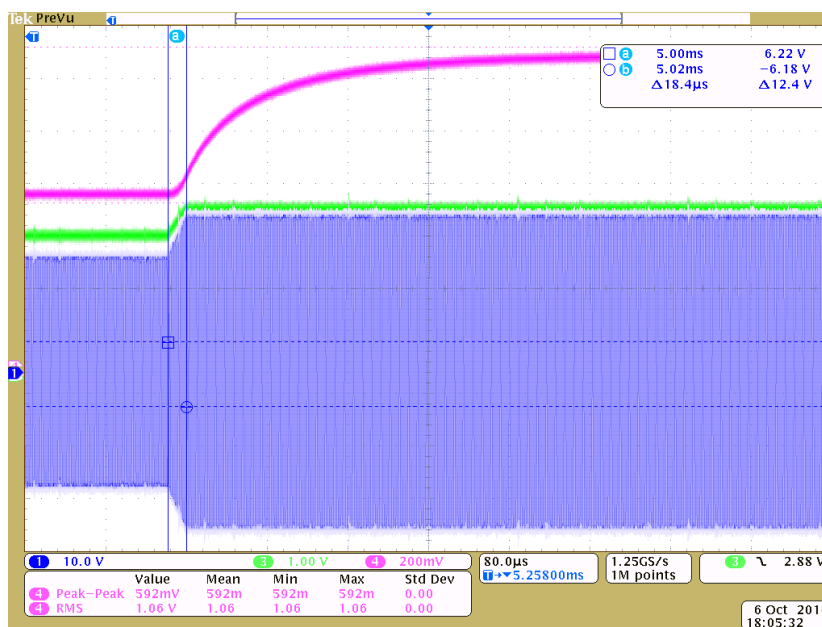


Fig. 09 Pink: power monitoring output (RF Driver), green: input signal, blue: RF amplitude. The power monitoring output simply stopped to behave normal but fortunately the RF amplitude is behaving as expected.

For the adjustment of the parameters an external disturbance was needed. One that is not in the same electronic circle but rather modifying the laser intensity somehow. This disturbing signal will then be compensated of the RP tuning the intensity of the dipole laser via RF Driver and AOM. While brainstorming with Niels we found about 7 ideas of which 5 included an electromotor. One of them was a rotating $\lambda/4$ -waveplate in order to create intensity fluctuations and another one was a fan with transparent rotor blades. Nevertheless, the best ideas was to simply put an LED next to the photodiode. The LED is driven by

a signal generator and therefore is blinking.

At a frequency of 1 kHz the optimized parameters were $K_P = 6500$ and $K_I = 8000$ (arbitrary units; those are integers between 0 and 8192).

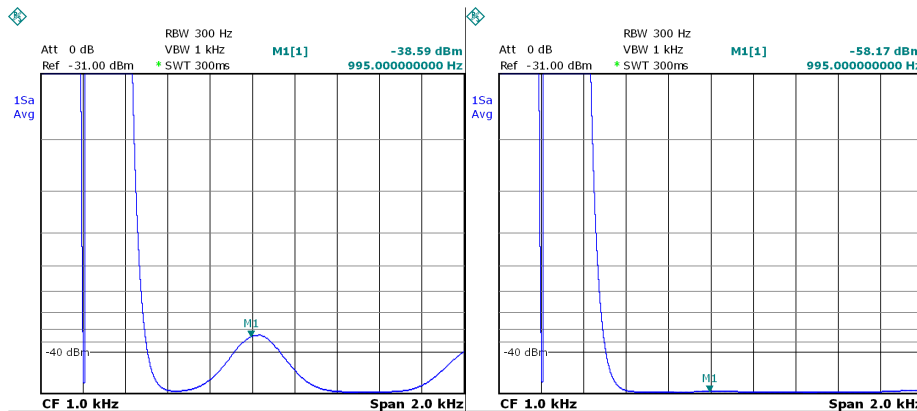


Fig. 10 Frequency spectrum of the set-up with the LED with-out (left) and with (right) the PID controller. The signal of the LED was compensated to the almost constant noise floor at -60 dBm.

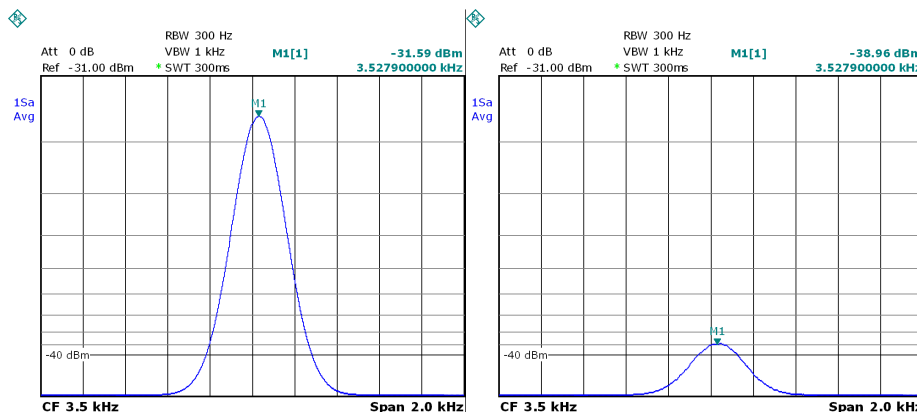


Fig. 11 Frequency spectrum of the same set-up with-out (left) and with (right) the PID controller. Here the signal at 3.5 kHz was still bigger than the noise floor.

When the LED was blinking at a frequency of 7.4 kHz, the phase difference between the signal of the photodiode and the RP output signal was already too high. You were able to see both signals oscillating but the peak on the spectrum

analyzer remained at the same height.

In the end it was the photodiode causing that huge delay, so it has been replaced by another one - PDA36A-EC. At this point it was no longer possible to add the DC offset voltage like shown in Fig. 06, because we put the ground of the Red Pitaya board to a potential of +4V against ground. Every measuring instrument and also the ground of the photodiode is grounded. The ground of every input and output of the RP board are connected. We then decided to build a summing amplifier.

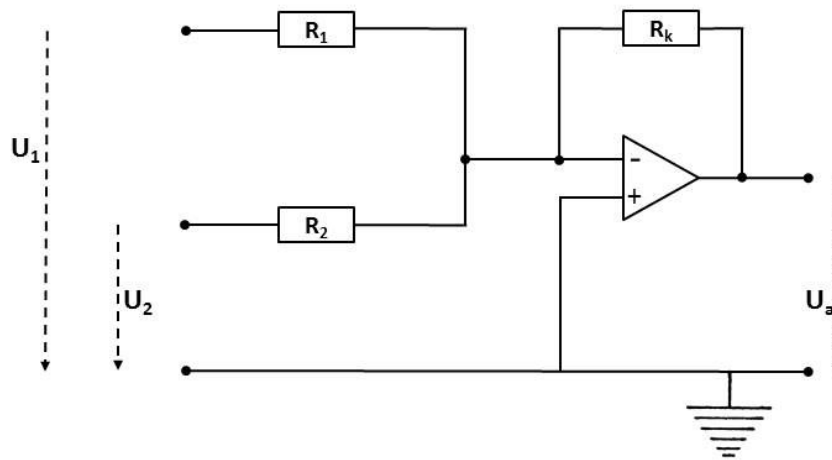


Fig. 12 Summing Amplifier. With $R_1 = R_2 = R_K$ we get $-U_a = U_1 + U_2$

Adding an inverting amplifier was reasonable.

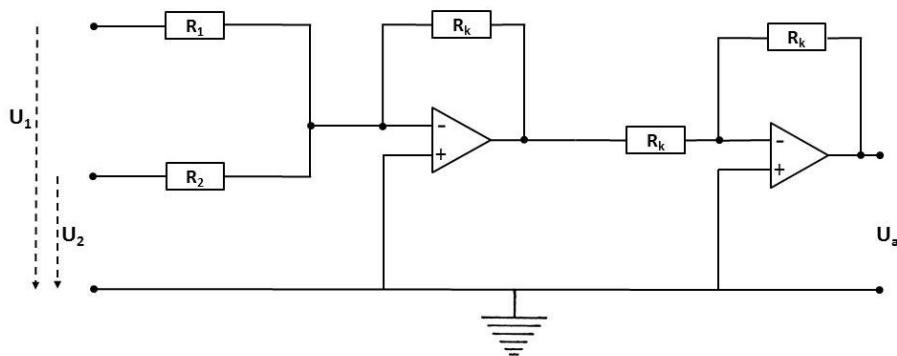


Fig. 13 Summing amplifier plus an inverting amplifier. With $R_1 = R_2 = R_K$ we now get $U_a = U_1 + U_2$.

Now the reaction time of the whole set-up has been reduced to $1.3 \mu s$. This delay was measured from the midpoint of the input signal to the midpoint of the output signal.

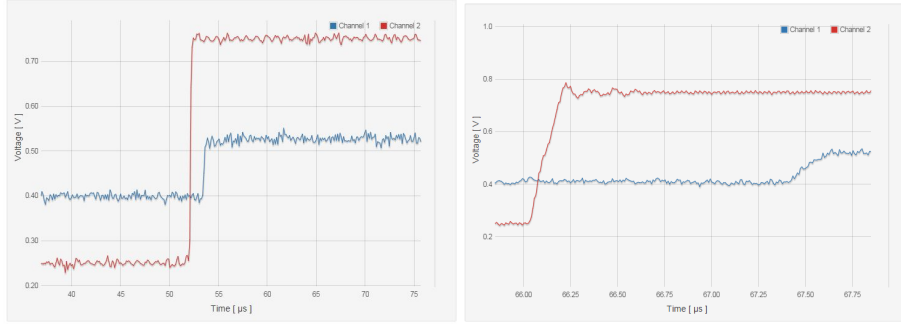


Fig. 13 Time delay between an incoming rectangular signal from the Red Pitaya (Channel 2) and the photodiode (Channel 1). The right diagram is the enlargement of the left one.

The rise time was no longer a problem and also the reaction time now is acceptable as we want to compensate noise up to a few hundred kHz.

In order to find the right parameters we again added optical disturbance to the dipole laser. This time the LED was not emitting enough intensity, because we replaced the photodiode and also had to replace the mirror from which the leakage has been used. The intensity incident on the photodiode now was 6 mW and at this point I am glad that there was no LED available with an intensity that high. We instead used the Zeeman Slower beam, which we modulated at a frequency f . The spectrum analyzer has been used to measure the peak at that frequency with and without the PID controller.

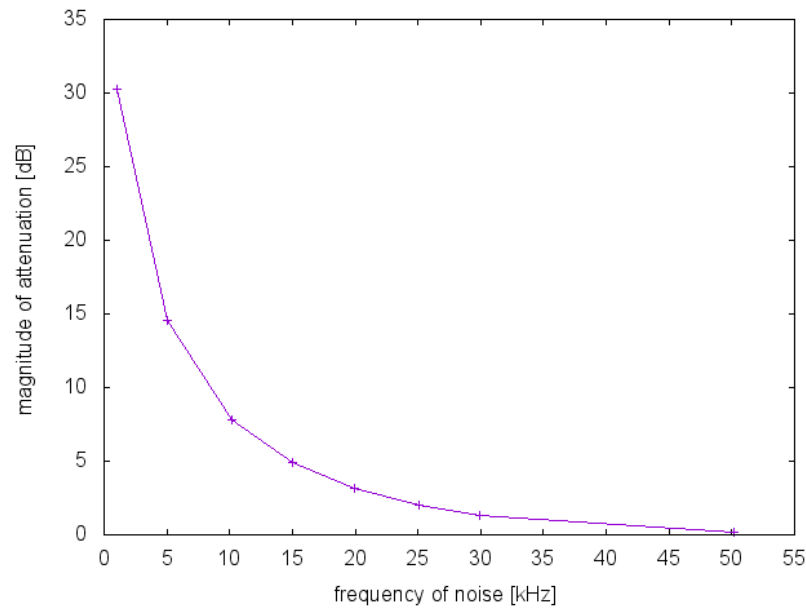


Fig. 14 Magnitude of attenuation vs frequency of noise. The Red Pitaya was able to compensate noise much better with the optimized setup, but it is still not good enough for the intensity stabilization of an optical dipole trap, because there is a peak at around 50 kHz in the natural noise spectrum of the dipole laser used here.

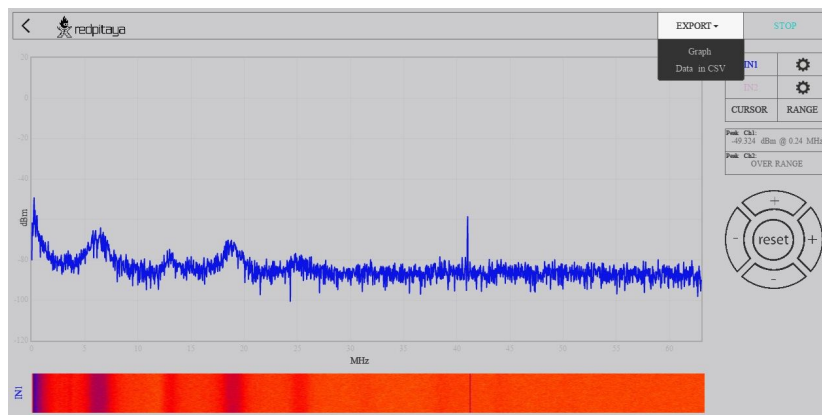


Fig. 15 Frequency spectrum of the laser intensity noise recorded by the Red Pitaya. The peaks coming from the dipole laser stand out against the noise floor coming from the cables, photodiode, etc.

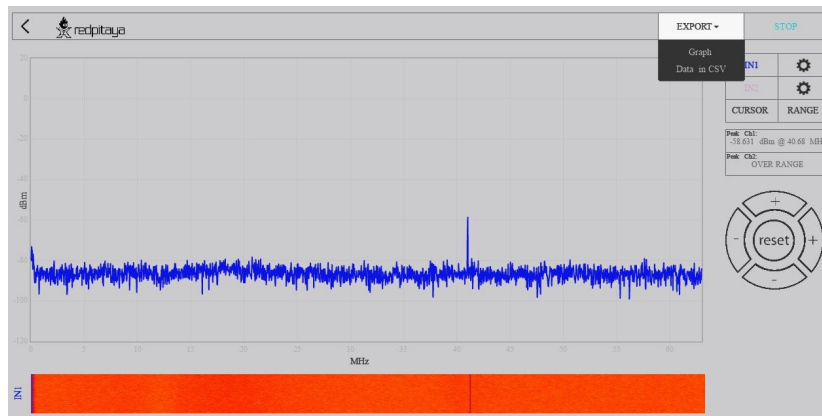


Fig. 16 Frequency spectrum of the noise floor. The peak at 40.68 MHz is induced from the BNC cable which connects RF Driver and AOM. This cable was probably too close to the cable for the input signal cable of the Red Pitaya.

The more interesting frequency range for our experiment is 1-100 kHz as noise in this regime affects the heating range the most. [14]

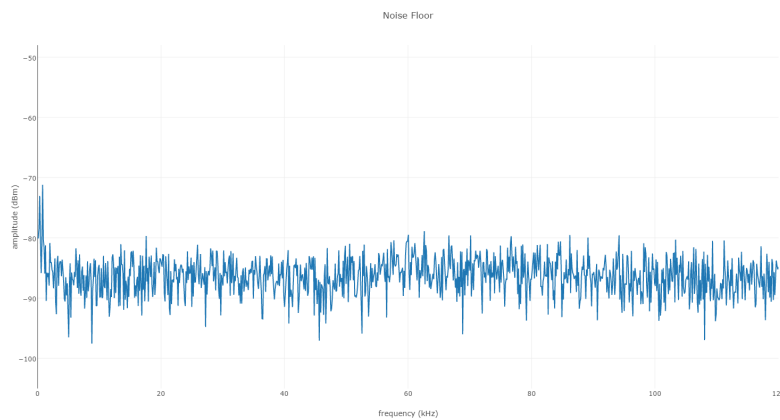


Fig. 17 Frequency range from 0.1-120 kHz of only the noise floor without the laser.

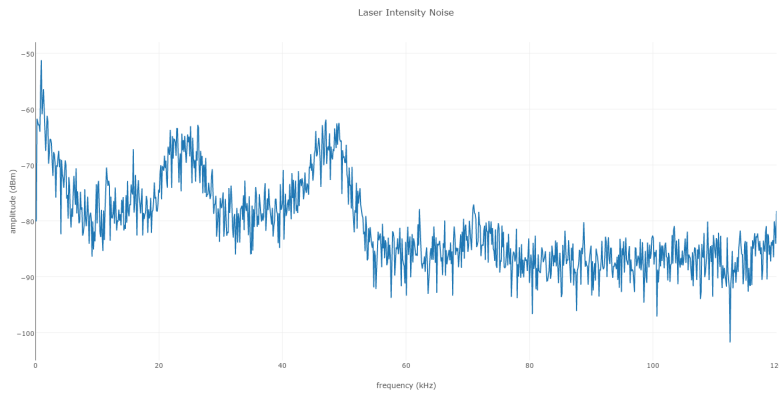


Fig. 18 Frequency range from 0.1-120 kHz. One big peak is at ~ 50 kHz where the Red Pitaya PID controller stops having an effect.

Another problem were overshoots on the output of the Red Pitaya. In the following figures the output signal of the Red Pitaya is shown - a rectangular signal with an amplitude of 20 mV_{pp} at different frequencies. A small amplitude was chosen, because the changes are as small when the PID control program is running. The following figures are on the same time scale.



Fig. 19 Overshoot from the RP output. Rectangular signal at 10 kHz.

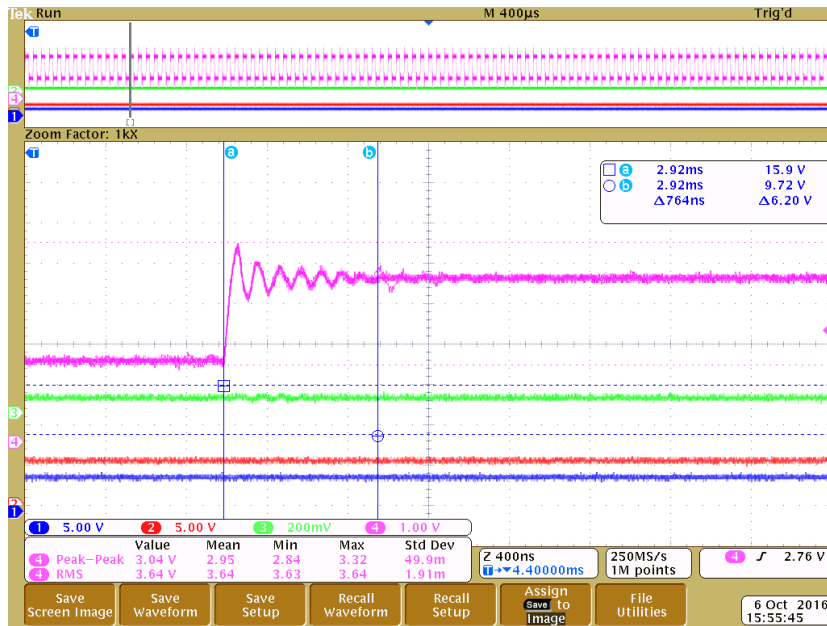


Fig. 20 Overshoot from the RP output. Rectangular signal at 25 kHz.

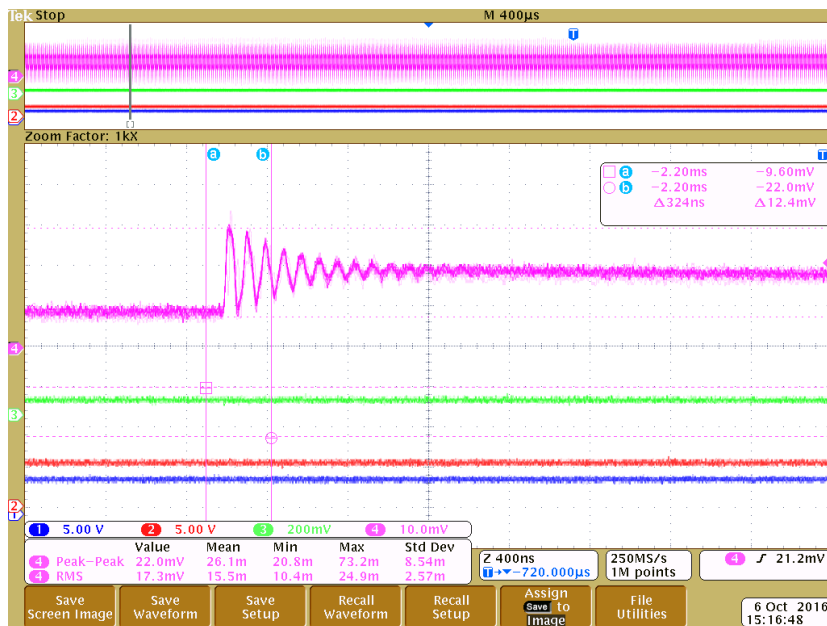


Fig. 21 Overshoot from the RP output. Rectangular signal at 100 kHz.

These overshoots bring additional noise to the laser frequency spectrum. This is another limiting factor of the Red Pitaya board as a PID controller. The other one is the reaction time of the RP - the time between an incoming signal and the output signal coming from the RP to compensate this edge. Maybe this software is not suitable for these rapid changes. One either has to write another software or which calculates the sum of the parameters faster or use another PID controller.

4.4 Analog PID Controller

Instead of using a digital controller it could be a better option to use an analog PID controller with rotary potentiometers instead of RP1, RC and RI in order to be able to change the control parameters for the optimization of the circuit.

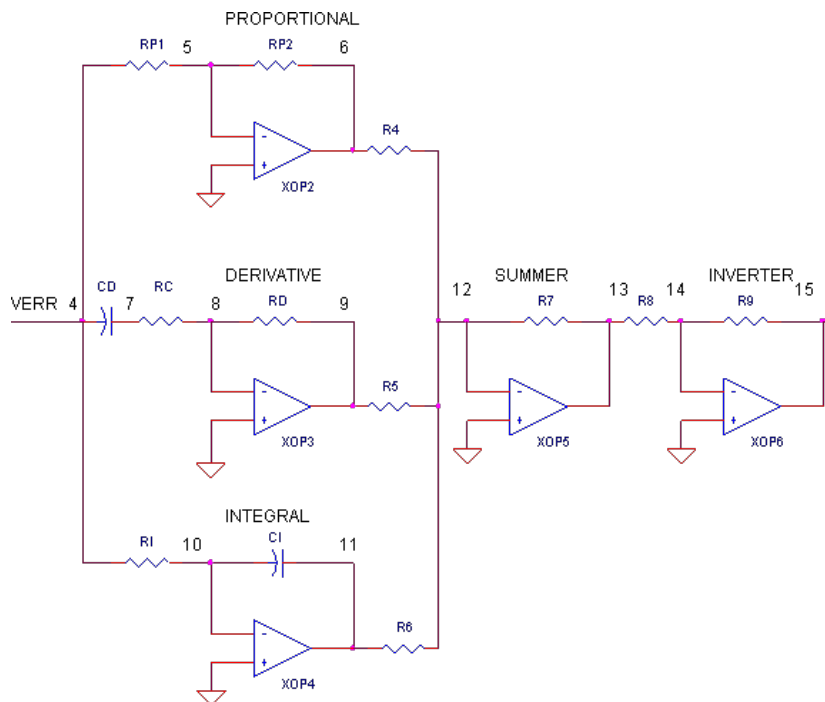


Fig. 22 Analog PID controller.²

It is important to check the dimensions of the resistors and capacitors precisely

²www.ecircuitcenter.com/Circuits/op_pid/op_pid.htm (17.10.2016)

in order to avoid lowpass and highpass filters. At least the important frequency range (0.1-500 kHz) for the stabilization should be let through. Analog PID controllers can also reach a short control time.

Since there were big issues with the intensity stabilization and we often got thrown back and had to start another attempt. Also the delivery time for the lenses (which will be discussed in the next chapter) was too long for analyzing them within the framework of this bachelor thesis.

Chapter 5

Possible Solutions

5.1 Thermal Lensing

In former experiments (dissertation of Thomas Lompe[3], dissertation of Matthias Kohnen[4]) Thermal Lensing has been a major issue. Due to the high laser power, the medium increases in temperature and therefore the shape of the beam changes. The beam waist increases, which changes the waist of the trap, where two crossed 80 μm -foci laser beams form a crossed dipole trap. Additionally the effective focal length increases, too, due to thermal effects. There is a thermal equilibrium after a certain time (order of magnitude μs to ms) but we can not make use of this effect because when loading the optical dipole trap from the MOT we first set the dipole laser to 200W and then ramp down the laser power to 30W, where the intensity stabilization will be conducted. The thermal effects get worse with increasing laser power so the focus shifts again while ramping down the laser power. A. Wenz and J. Stachurska from the work group of S. Jochim (Heidelberg) analyzed the quantity of these effects quite detailed.

One option is to use optics with a low absorption coefficient and a low thermal expansion coefficient, such as Fused Silica. In the following table Thorlabs BK7 [10] and Corning HPFS (High Purity Fused Silica) [11] are compared for their absorption and their thermal coefficient.

	Absorption	Thermal Coefficient
@1070nm	[ppm/cm]	[$10^{-6}/K$]
Thorlabs BK7	~ 1000	8.3
Corning HPFS 7980 Standard Grade	≤ 30	0.58
Corning HPFS 7979 Infrared Grade	≤ 10	0.58

Tab. 02 Specifications for the often used Thorlabs BK7 and Corning HPFS.

	Homogeneity	Metallic Impurities	OH Content
@1070nm	[ppm]	[ppb]	[ppm]
HPFS 7980 Standard	≤ 0.5	< 1000	800 – 1000
HPFS 7979 Infrared	≤ 0.5	< 100	< 1

Tab. 03 Specifications for Corning HPFS

In these data sheets it is often referred to the *Internal Transmittance* which is the same as 1-Absorption. In most data sheets there is only a value for the *Transmittance* where also includes energy loss due to scattering, reflection, etc. Most companies also do not take into account that the AR Coating also absorbs a part. The AR Coating used at the company *II-VI Infrared* absorbs ≤ 3 ppm on each side (typical values are 1.5 ppm).

The OH content means the number of atoms or molecules with a hydroxy group. This hydroxy group absorbs photons in the infrared regime quite well. Fused Silica (SiO_2) always contains parts of silanol ($SiOH$). Also metals can absorb infrared light. Low values therefore are no harm. Also one should try to illuminate the whole lens and not just the center of it.

In our beam path (Fig. 23) the illumination of the whole lens is possible for every one but the first two of them. The first two lenses form a telescope to decrease the beam diameter from 5 mm (coming from the laser head) to 2.5 mm (where the AOM works fine). If you move the second lens ($f = -125$ mm) is slightly moved closer to the first lens, the beam diverges faster than it would for a distance of 125 mm. There then is a segment directly behind the second lens where the beam is almost parallel (without divergence) : The beam diameter

increases over the 52 mm (thickness of the crystal in the AOM) just by a few ‰. Then again the distance between the second and the third lens has to be about 670 mm so that the beam diameter is big enough. I simulated this beam path with GaussianBeam. I tested if this beam path would be possible in order to minimize the number of optical elements.

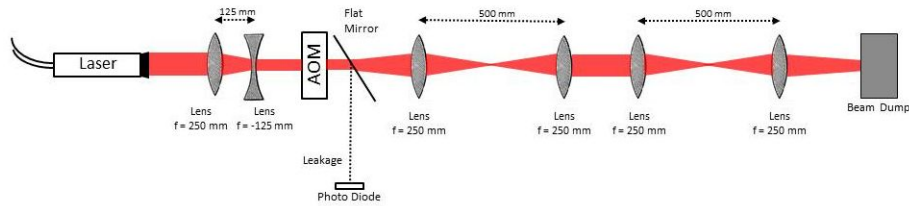


Fig. 23 Beam Path.

Otherwise it could be the better idea to just add a second telescope after the AOM. The concave lens has a center thickness < 5 mm, which should not affect the beam that much. Planned is an optical dipole trap consisting of a crossed beam with an angle of incidence $\alpha = 5^\circ$ (the highest possible angle for this geometry: diameter of the windows = 32 mm, diameter of the vacuum chamber = 436 mm). So the beam diameter is also a limiting factor for α .

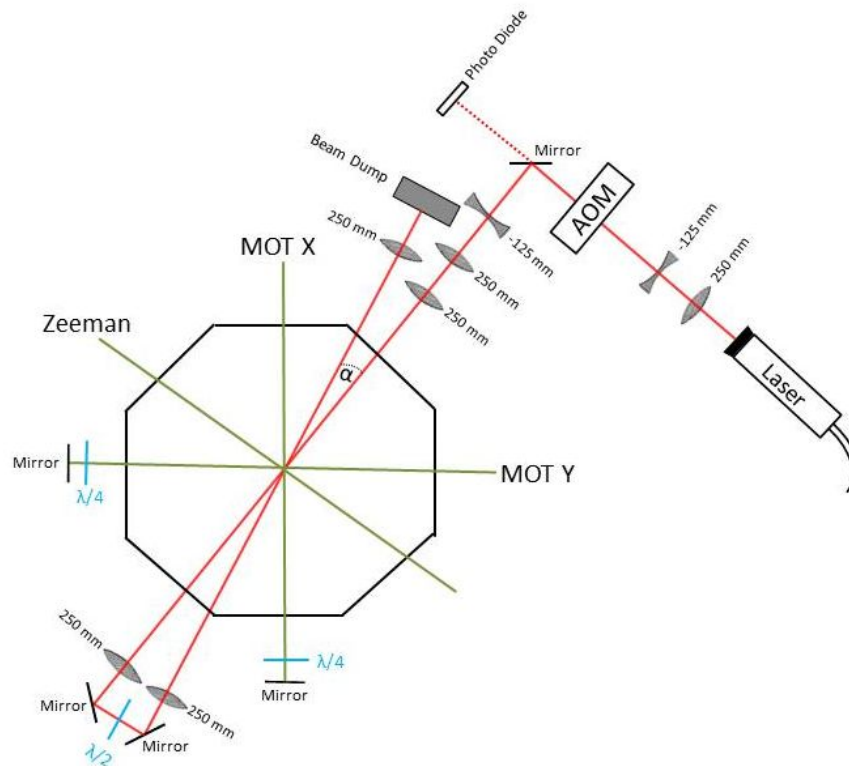


Fig. 24 Beam path through the chamber. The convex lenses all have $f = 250 \text{ mm}$ and the concave lenses have $f = -125 \text{ mm}$.

Another idea was to use spherical mirrors. But they need to be at a 45° -geometry since I only found mirrors which reflect the beam like this.

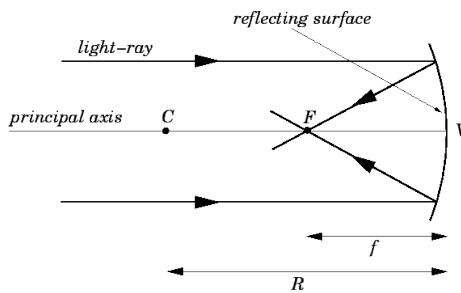


Fig. 25 Concave mirror.¹

¹<http://farside.ph.utexas.edu/teaching/3021/lectures/node136.html>

This geometry is rather useless since the beam therefore would have to travel through the chamber without being focussed first. Spherical mirrors working at a angle of incidence $\beta = 45^\circ$ would be a good choice since the absorption would be much smaller because the light does not have to travel through a medium.

Bibliography

- [1] Grimm, R., Weidemüller, M., & Ovchinnikov, Y. B. (2000). Optical dipole traps for neutral atoms. *Advances in atomic, molecular, and optical physics*, 42, 95-170.
- [2] Seidler, F., (2015). Digital high bandwidth feedback controller. Master thesis.
- [3] Lompe, T., (2011). Efimov Physics in a three-component Fermi gas. Dissertation.
- [4] Kohnen, M., (2008). Ultracold Fermi Mixtures in an Optical Dipole Trap. Dissertation.
- [5] Wenz, A., Stachurska, J. (2012). Notes on: Thermal Lensing with high intensity cw Lasers.
- [6] Schuricke, M., (2012). Two and Three Photon Double Ionization of Lithium. Dissertation.
- [7] <http://pegasus-optik.de/PDF/MQ40-A2-A3-W.pdf> (17.10.2016)
- [8] <http://www.pegasus-optik.de/PDF/QMODP1-02.pdf> (17.10.2016)
- [9] http://www.ipgphotonics.com/laser/view/128/Lasers/Mid_Power_CW_Fiber_Lasers/1__m/YLR_LF (17.10.2016)
- [10] http://www.schott.com/advanced_optics/german/abbe_datasheets/schott-datasheet-n-bk7.pdf (17.10.2016)
- [11] https://www.corning.com/media/worldwide/csm/documents/HPFS%20Product%20Brochure%20All%20Grades%202013_08_15.pdf (17.10.2016)

- [12] <http://www.iivinfrared.com/1-Micron-Optics-Materials/fused-silica-aspheres.html> (16.10.2016)
- [13] https://www.dropbox.com/s/b2pxkwj1ljzyw71/Red_Pitaya_HW_Specs_V1.1.1.pdf (16.10.2016)
- [14] Savard, T. A., O'hara, K. M., & Thomas, J. E. (1997). Laser-noise-induced heating in far-off resonance optical traps. *Physical Review A*, 56(2), R1095.
- [15] <http://www.adwin.de/de/produkte/proII.html> (17.10.2016)

Acknowledgements

After five fascinating months of research, studying and also quite a lot of fun while working on the chamber I would like to thank the following people:

- Niels Kurz for his guidance, advice and his motivation after something terribly failed.
- Priv.-Doz. Dr. Alexander Dorn for his help and advice and also the opportunity to work on such a practical experiment.
- Prof. Dr. Thomas Pfeifer for acting as second referee.
- Janko Nauta for his help with the usage of the Red Pitaya board and the PID control software.
- The whole Pfeifer Division for the sympathique working atmosphere.

Erklärung

Ich versichere, dass ich diese Arbeit selbstständig verfasst und keine anderen als die angegebenen Quellen und Hilfsmittel benutzt habe.

Heidelberg, den 18.10.2016